Comparing pre- and post-construction distributions of long-tailed ducks *Clangula hyemalis* in and around the Nysted offshore wind farm, Denmark:

a quasi-designed experiment accounting for imperfect detection, local surface features and autocorrelation

IB KRAG PETERSEN[1], MONIQUE MACKENZIE[2], ERIC REXSTAD[3], MARY S. WISZ[4], ANTHONY D. FOX[1]

[1]*Department of Wildlife Ecology and Biodiversity, National Environmental Research Institute, Aarhus University, Grenåvej 14, DK-8410 Rønde, Denmark*

[2]*Centre for Research into Ecological and Environmental Modelling, University of St. Andrews, St. Andrews KY16 9LZ, United Kingdom*

[3]*Research Unit for Wildlife Population Assessment, Centre for Research into Ecological and Environmental Modelling, University of St. Andrews, St. Andrews KY16 9LZ, United Kingdom*

[4]*Arctic Environment Department, National Environmental Research Institute, Aarhus University, Frederiksborgvej 399, PO Box 358, DK-4000 Roskilde, Denmark*

Abstract: We report a novel technique to model abundance patterns of wintering seaducks in relation to the construction of an offshore wind farm (OWF) based on seven years of aerial survey transect data. Distance sampling was used to estimate seaduck densities adjusted for covariates affecting detection probabilities. A generalized additive model (GAM) generated seaduck densities in sampling units in relation to spatially explicit covariates, using bootstrapping to account for uncertainties in both processes. Generalized estimating equations generated precision measures for the GAM robust to spatial and temporal autocorrelation. Comparison of pre- and post-construction model generated surfaces showed significant reductions in long-tailed duck numbers only within the OWF (despite the fact that the model was uninformed about the OWF location), although the absolute numbers involved were trivial in a flyway population context. This method provides quantification of distributional effects on organisms over a gradient in space and time that offers an alternative to Before-After/Control-Impact designs in environmental impact assessment.

Key words: Aerial surveys; distance sampling; environmental impact assessment; feeding densities; generalized additive models; parametric bootstrap; spatially-adaptive model; generalized estimating equations; seaducks; spatial autocorrelation; temporal autocorrelation.

INTRODUCTION

Methods for detecting distributional effects on wildlife populations associated with major construction projects have traditionally been based on "quasi-experiments" that track animal distribution and abundance through time in relation to anthropogenic factors. For example, BACI (before/after control/impact)-type designs (Green 1979, McDonald et al. 2000, Smith 2002) compare numbers in modified/impacted areas with those in a control area before and after the impact. Heterogeneous landscapes constrain options for defining control areas that sufficiently resemble the impact area, compounded by lack of adequate control/impact replication (Underwood 1991). Ideally, we wish to compare changes in animal abundance (compiled at fine spatial resolutions) along a gradient to the center of an alleged impact zone to define spatial responses (Guillemette and Larsen 2002). Line transect surveys present a rich source of animal location information that can be used to derive animal abundance estimates which can be analyzed using distance sampling (Buckland et al. 2004) and spatial modeling tools (Hedley and Buckland 2004) to quantify how abundance patterns change with time and space in relation to an alleged impact at fine spatial resolution. In this paper, we couple distance sampling methodology with novel modeling tools to derive spatially explicit estimates of long-tailed duck abundance in relation to the Nysted Offshore Wind Farm (OWF) in southern Denmark. Specifically, we compare temporally averaged duck abundance before and after installation of the turbines and its spatial pattern in relation to the OWF (see Fig. 2 in Fox et al. 2006 for conceptual framework).

METHODS

Study Area

Nysted OWF lies 10 km southwest of Gedser in Femern Belt (Fig. 1), c.4 km south of the Rødsand sandbar which runs c.25 km from Hyllekrog to Gedser. Water depth in the wind farm varies between 6 m and 9.5 m over glacial sand/silt sediments with aggregations of pebbles, gravel and shells. The water is brackish and the lunar tide is weak (less than 0.5 m, water level variation is mainly determined by wind). A busy shipping lane lies just south of the OWF, fishery and recreational boats of all sizes use the area outside the OWF in summer. The current Nysted OWF consists of 72 2.3 MW wind turbines, arranged in a trapezoid of 8 rows of 9 covering an area of 24 km^2 (Fig. 1). Turbine nacelles are situated 69 meters above mean sea level and rotor blades are 41 meters long, giving a total height of 110 meters. Almost all turbines were erected in summer/autumn 2002, so throughout, "pre-construction" refers to January-April 2000-2002 inclusive and "post construction" 2003-2007.

Survey Area and Data Collection

The 1,350 km^2 surveyed study area was defined to cover the Nysted OWF site and a large reference area around, representing a bio-geographical unit for wintering long-tailed ducks (Fig. 1, Petersen et al. 2006). Within each winter season (January to early April) from 2000 to 2007 (excepting 2006) three or four surveys were conducted from a high winged, twin-engined Partenavia P-68 Observer reconnaissance aircraft at 76 m above sea level (measured by onboard radar altimeter) at 185 km/h (100 knots) along 26 pre-defined north-south transects at 2 km intervals (total track length 579 km, Fig. 1). Two trained observers (familiar with species identification) scrutinized each side of the aircraft instantaneously recording all observations of all avian species, number, behavior, perpendicular distance from track line and time onto a Dictaphone. Behaviors were recorded as sitting (on water), diving, flushing or flying. Observations were binned into three transect bands defined by perpendicular distance from the survey track line, each determined using an inclinometer (predetermined angles of 4º, 10º and 25º below the horizontal measured abeam). A band 44 m out on each side of the flight track directly below the aircraft was not visible to observers. The inner, middle and outer transect bands were 119 m, 269 m and 568 m wide respectively. Only long-tailed duck observations are considered here.

Survey flight tracks were logged by computer from a differential GPS at five second intervals, recording longitude/latitude (to c.2 m accuracy) and time. On the extremely rare occasions of GPS failure, bird observation positions were calculated from the known time of passage at the navigation way points and interpolated from the aircraft cruising speed, inevitably compromising observational spatial accuracy. The majority of observations were considered to be accurate to within four seconds, which with a flight speed of 185 km/h gives a positional accuracy to within 206 m, at high bird densities, positional accuracy may rarely have fallen to 515 m (10 seconds observational delay).

Surveys were never carried out when wind speed exceeded 6 m sec^{-1}, when detectability of birds was severely reduced. In severe glare, observations from one side of the aircraft were temporarily discontinued. A surface covering GIS bathymetry layer was established from point-based high resolution multi-beam data made available from the Danish Maritime Safety Administration.

Total study area abundance estimates over time

The total numbers of long-tailed ducks found in the study area was estimated for each of the surveys using conventional distance sampling to correct for detectability, not subject to spatial modeling of covariates. Model selection and the results from this estimation exercise are presented in Appendices A & B.

Fine scale abundance estimates over time

The primary goal was to model fine-scale abundance patterns of long-tailed ducks over time in relation to the construction of the wind farm in a manner that reflected environmental heterogeneity in the study area, accounting for important sources of uncertainty. To achieve this we combined methods for fitting detection functions with a spatially-adaptive generalized additive model (GAM) and generalized estimating equations (GEEs) (Hardin and Hilbe 2003). Distance sampling was used to estimate long-tailed duck density from transect data, using detection functions to adjust these estimates in relation to factors influencing the ability of observers to detect them (e.g. distance from observer, sea state, group size etc, Buckland et al. 2004). The detection function portion of this analysis was used to estimate long-tailed duck densities in fine scale sampling units (i.e. 500 m segments) as a function of covariates expected to affect an observer's ability to detect ducks. The spatially-adaptive GAM model related these abundance estimates in sampling units to spatially-explicit covariates. Bootstrapping allowed us to account for the various uncertainties arising from selecting the detection function, and fitting of the spatially-adaptive GAM. The GEEs produced measures of precision for the GAM which are robust to spatial correlation (Hardin and Hilbe 2003) inherent in line transect data and were used to ensure parameter uncertainty in the face of autocorrelation was realistic.

Estimating abundance along the transect lines (0.5 km segments)

Using all the survey data, we fitted a suite of plausible detection functions supported by Petersen et al. (2006) that included various combinations of relevant covariates, and identified the most parsimonious among these using AIC. Hazard function and half normal key functions were considered, as were the most plausible combinations of the covariates observer, bird behavior, sea state, flock size, survey (surrogate for date) and pre-construction/post-construction phase of the study (see Appendix A). Each survey transect was divided into segments 0.5 km in length, with a width equal to twice the truncation distance. We then used the most parsimonious detection function among these to estimate the number of seaducks in each segment using the count method of Hedley and Buckland (2004). This method uses the Horvitz-Thompson estimator to calculate counts per segment as the sum of the inverse of the probability of detection for all observations in each segment.

Modeling the spatial distribution of long-tailed ducks pre- and post wind farm construction: spatially-adaptive generalized additive model

The abundance estimates obtained using distance sampling were modeled using a spatially-adaptive quasi-Poisson errors based, generalized additive model (GAM, Hastie and Tibshirani 1990) with an offset. The model included a one-dimensional smooth term for depth and a spatially-adaptive two dimensional smooth term for the X/Y coordinate based spatial surface. These smooth relationships were permitted to differ before and after construction in both shape and magnitude using construction-based interaction terms. The linear predictor for the general model can be written as:

$$\eta_{it} = \beta_0 + s_1(Depth_{it}) + s_2(X_{it}Y_{it}) + construction_{it} + s_3(Depth_{it})construction_{it} + s_4(X_{it}Y_{it})construction_{it} + \log(area_{it})$$

where η_{it} represents the linear predictor for segment *i* at time *t*, β_0 is the intercept parameter, s_1 and s_3 are one-dimensional smooth terms representing the depth relationship before and after construction respectively, while *construction* refers to the "before" and "after" time periods 2000-2002 and 2003-2007. s_2 and s_4 are spatially-adaptive two-dimensional smooth terms representing the spatial distribution of long-tailed ducks before and after construction respectively. Differences in the distribution before and after construction are of particular interest because any wind farm related effects might be reasonably expected to decline with the distance from the wind farm. Area is an offset measuring the effective size of the segment of sea sampled.

The smooth functions for depth were specified to be cubic *B*-splines while the two-dimensional smooth functions are represented by radial basis functions with a fixed number of 'space-filled' knots. The space-filling approach uses an efficient design which maximizes the distance between knots to obtain good coverage across the modeling surface (Johnson et al. 1990). These radial basis functions were specified to accommodate local surface features by determining a radius (*r)* for each knot that contains a fixed proportion of the survey data. This spatially-adaptive approach permitted the radii to vary locally across the surface so that data-sparse areas exhibit larger radii and approximate relatively global changes in the surface while data-rich areas exhibit smaller radii and can approximate local surface features. The k^{th} column of the radial basis matrix can be written as:

$$d_{kit} = \exp\left(\frac{-(\| x_k^* - \mathbf{x}_{ti} \|)^2}{r_k^2}\right)$$

where d_{kit} represents the Euclidean distance between the spatial coordinates for the observed data ($\mathbf{x}_{it}$) and the x,y coordinate (x_k^*) for knot location *k.* The radius denominator r_k^2 represents the square of the radius (*r*) allocated to knot location *k*.

These distances are used to make the two-dimensional smooth functions and feature in the linear predictor in the following way:

$$\eta_{it} = \beta_0 + \sum_{p=1}^{P} \beta_p (Depth_{it}) + \sum_{k=1}^{K} \beta_{(P+k)} d_{kit} + \beta_{(P+K+1)} C_{it} + \sum_{q=1}^{Q} \beta_{(P+K+1+q)} (Depth_{it}) \times C_{it} + \sum_{k=1}^{K} \beta_{(P+K+1+Q+k)} d_{kit} \times C_{it} + \log(area_{it})$$

where the *p=1,…,P* and *q=1,…,Q* coefficients represent the cubic *B*-splines for depth before (2000-2002) and after (2003-2007) construction (represented by the binary variable C_{it} *)* respectively, the *k=1,…,K* coefficients represent the spatial surface with locally varying *r*, before and after construction (one coefficient per knot location *k*).

Modeling the spatial distribution of long-tailed ducks pre- and post wind farm construction: generalized estimating equations

The data comprise repeat visits to transects over time, and so residual independence within transects was unlikely. For this reason, generalized estimating equations (GEEs; Hardin and Hilbe 2003) were used to generate more realistic model standard errors and 95% confidence intervals for model-based differences before and after construction.

The 'panels' (or 'subjects') for the GEEs were chosen to be transect-days by inspection of autocorrelation functions using Pearson residuals; i.e. residuals within transects on a given day were permitted to be correlated, but independence was assumed between transects on a given day. Additionally, residuals for transects in the same spatial location visited on different days were assumed independent. The validity of these assumptions will be examined in light of model results. Empirical standard errors were used to generate model standard errors (Halekoh et al, 2006), to help ensure robust estimates of precision.

Model Selection

The number of knots used for the two-dimensional surface and the proportion of the data (*p*) used to determine the radius of each knot was chosen using a cross-validation exercise. The cross-validation exercise involved randomly omitting 30% of the transect-days using a range of *p* (0.01-0.3 in 0.01 increments) to determine r_k across a range of space-filled knot schemes (10-40 knots). The sum of the squared errors when comparing the predictions under each model to the out-of-set data and the observed out-of-set data was then calculated for each knot scheme and *p* to give a cross-validation score. The knot number was then chosen using the lowest average CV score across the knot sets. The ranges trialed for *p* and the number of knots were chosen using a pilot cross-validation scheme prior to the cross-validation analysis.

The number of internal knots used for the smooth depth relationship was also chosen using a CV analysis (similar to that described above) following the CV-based specification of the spatial smoother. This CV analysis trialed between 1 and 10 internal knots as a part of the CV process and the number of internal knots with the lowest average CV score was chosen.

Combining uncertainties

The uncertainty in the detection process and parameter uncertainty in the GAM-GEE model was combined using a two-step bootstrap approach. Five hundred non-parametric bootstrap realizations were used to summarize uncertainty from the detection process and the GAM-GEE model was refitted to each realization. The GAM-GEE based estimates and corresponding standard errors from this stage were then used to generate 1000 parametric bootstrap realizations for each of the resulting realizations. This lead to 500,000 predictions for each cell across a prediction grid comprised of cells of 0,966 km^2. For each set of predictions, the differences between estimated long-tailed duck numbers pre-construction and post-construction across the prediction grid were found and 95% confidence intervals (based on percentiles) for these differences were harvested (see Appendix C).

RESULTS

Detection function modeling and broad scale abundance estimates

Appendix A shows the model selection results for fitting detection functions to the aerial survey data in the fine-scale analysis. The close contest between the top two candidate models shows there to be considerable uncertainty about the detection function most appropriate for these data, however most of the covariates offered for inclusion in the models appeared in the preferred model. The most parsimonious detection function across surveys included the following covariates: sea state, scaled flock size, behavior, and observer. When this detection function was fitted to each survey across the entire study area, more long-tailed ducks were estimated in the April 2002 survey than in any other (Appendix B).

Modeling spatial distribution of long-tailed ducks before and after wind farm construction

Under the cross-validation scheme, 38 knots were chosen with radii which captured 4% (p=0.04) of the survey data nearest to each knot location. The CV analysis also selected a smooth term for 'Depth' with 2 internal knots. The model-based results were used to generate an after-before surface which indicates an estimated drop in long-tailed duck numbers around the wind farm with an apparent displacement into neighboring waters further from the wind farm. The magnitude of the changes were small on average; the largest negative estimated difference was -3.00 individuals per segment and the largest estimated positive difference was 9.54 individuals per segment across the prediction grid (Fig. 1). Despite the uncertainty about model predictions after considering both the detection and modeling processes, there was evidence for significant decreases in long-tailed duck numbers only in survey grid cells between the turbines and significant increases in waters further away (Fig. 1).

The extent of the within transect-day correlation was estimated to be small (for example, the estimated correlation coefficient under an AR(1) process=0.1536), but the practical consequences of incorporating the non-independence within transect-days were marked. The GEE-based standard errors were between 4.5 and 17.0 times the size of the standard errors obtained under independence (similar to the findings of Lapena et al. (2010)). The residual autocorrelation was estimated to decay very quickly along transect segments (on a particular day) and residuals just three units (500 m) apart are effectively independent under the model; the correlation coefficient under an AR(1) model for residuals three units apart was estimated to be 0.003624). In light of this, the assumption that transects 2 km apart are independent is reasonable. Additionally, inspection of Pearson's residuals revealed negligible correlation for revisits to the same transects on different days.

DISCUSSION

A long established challenge to ecologists is to find reliable and cost-effective means for measuring distributional effects of geographically discrete human development projects on natural populations. Traditional BACI-type studies, such as those associated with a single development (e.g. wind farms), inevitably compare "impacts" between un-replicated impact and control sites (Stewart-Oaten et al. 1986, Underwood 1991). Changes in distribution and abundance of study organisms at such sites may differ through time by chance and finding ecologically identical areas differing only in exposure to human impact at appropriate scales and degree of separation is impossible, leaving this approach vulnerable to criticism. Designed experiments offer a credible means to test the potential impact of human disturbance on animal populations, but count-based changes in abundance or density are insufficient for defensible impact assessment. The uncertainty associated with estimating animal abundance when detection is imperfect presents challenges in impact assessment, but these can be overcome using methods presented here. We demonstrate that propagating the uncertainty associated both with modeling of the detection process, as well as modeling of the impact can be done using bootstrap methods to resample the data and subject bootstrap samples to both modeling steps. In this case we have modelled the impact using a 'change surface', with other covariates (such as bathymetry) that potentially influence the distribution of seaducks, which is a seamless way to examine the strength of the impact, in the presence of other biologically relevant factors.

In this study, long-tailed duck density estimates could be predicted by the depth relationship and a spatial surface before and after construction, which permitted any changes before and after impact to differ with direction from the wind farm.

For analyses like these, the recognition of non-independence in model residuals is crucial to ensure sampling variability based fluctuations in abundance are not mistaken for genuine impact effects (Lapena et al, 2010). In this case the GEE-based standard errors were many times higher than the independence-based standard errors which would likely have led us to conclude that many more cells on the prediction grid exhibited significantly different abundances post-impact.

Density estimates were only statistically significantly higher pre-construction within the confines of the OWF compared to post construction, despite the fact that the model was totally uninformed about the OWF location (Fig.1). Although long-tailed ducks occurred between the turbines, the model estimated they did so at lower densities. This evidence suggests that there has been some displacement of long-tailed ducks after construction of the wind farm, despite the fact that the number of birds did not appear to have changed in the general area post-construction (Appendix B). It is not yet possible to attribute the redistribution of long-tailed ducks at Nysted to (i) avoidance of turbines, (ii) disturbance from increased maintenance traffic, (iii) changes in food supply or (iv) predators, or a combination of these and other causes. Further investigations should be carried out to see if other biotic covariates (such as benthic sediment type and prey availability) could better resolve patterns of abundance in long-tailed duck relative to the OWF.

Part of our inference about the effect of the wind farm is derived from our spatially-explicit estimates of predicted density within 0.5 km transect segments, and we found that the uncertainties associated with these predicted densities varied considerably with distance from the wind farm both pre- and post-construction.

The number of long-tailed ducks directly impacted by this development was trivial (4-5 long-tailed ducks per survey segment) relative to the total flyway population size (4.6 million individuals, Delany and Scott 2006). Although we know little about the potential impacts of such displacement (in terms of the interference or depletion competition effects experienced by birds displaced from the vicinity of the wind farm to forage elsewhere), it seems unlikely that the construction of this wind farm will have any detectable effect at the population level.

ACKNOWLEDGEMENTS

We thank NERI colleagues, especially Mark Desholm, Johnny Kahlert, Thomas Kjær, Ib Clausager, Karsten Laursen and Henning Noer, the Danish Wind Farm International Expert Panel, DONG Energy (especially Charlotte Boesen, Pernille Holm Skyt, Steffen Andersen and Per Hjelmsted Pedersen) and members of the Environment Group for guidance and funding to undertake this study. We acknowledge finance for elements of this work from the Danish Public Service Obligation Funds and the Danish Strategic Research Council.

LITERATURE CITED

Buckland, S.T., Anderson, D.R., Burnham, K.P., Laake, J.L., Borchers, D.L., and Thomas, L. 2004. Advanced Distance Sampling. Oxford University Press, Oxford, UK.

Delany, S. & Scott, D. 2006. Waterbird Population Estimates – Fourth Edition. Wetlands International, Wageningen, The Netherlands.

Fox, A.D., Desholm, M., Kahlert, J., Christensen, T.K. and Petersen, I.K. 2006. Information needs to support environmental impact assessment of the effects of European marine offshore wind farms on birds. Ibis 148:129-144.

Green, R. H. 1979. Sampling design and statistical methods for environmental biologists. Wiley Interscience, Chichester, UK.

Guillemette, M., and Larsen, J.K. 2002. Post-development experiments to detect anthropogenic disturbances: the case of sea ducks and wind parks. Ecological Applications 12:868–877.

Halekoh, U., Højsgaard, S., and Yan, J. 2006. The R package geepack for generalized estimation equations. Journal of Statistical Software 15(2):1-11.

Hardin, J., and Hilbe, J. 2003. *Generalized Estimating Equations.* Chapman and Hall/CRC, London, UK.

Hastie, T., and Tibshirani, R. 1990. *Generalized Additive Models*. London: Chapman and Hall/CRC, London, UK.

Hedley, S.L., and Buckland, S.T. 2004. Spatial models for line transect sampling. Journal of Agricultural, Biological and Environmental Statistics 9:181-199.

Johnson, M.E., Moore, L.M., and Ylvisaker, D. 1990. Minimax and maximin distance designs. Journal of Statistical Planning and Inference 26:131-148.

Lapena, B. P., Wijnberg, K.M., Hulscher, M.H., and Stein, A. 2010. Environmental impact assessment of offshore wind farms: a simulation based approach. Journal of Applied Ecology, 47: 1110-1118.

Maar, M. Bolding, M., Petersen, J.K., Hansen, J.L.S., and Timmermann, K. 2009. Local effects of blue mussels around turbine foundations in an ecosystem model of Nysted off-shore wind farm, Denmark. Journal of Sea Research 62:159-174.

McDonald, T.L., Erickson, W. P., and McDonald, L. L. 2000. Analysis of count data from before-after control-impact studies. Journal of Agricultural, Biological, and Environmental Statistics 5:262-279.

Petersen, I.K., Christensen, T.K., Kahlert, J., Desholm, M., and Fox, A.D. 2006. Final results of bird studies at the offshore wind farms at Nysted and Horns Rev, Denmark. Report to Dong Energy and Vattenfall A/S, National Environmental Research Institute, Rønde, Denmark.

Smith, E.P. (2002) BACI design. Pages 141-148 *in* A.H. El-Shaarawi, and W.W. Piegorsch, editors. Encyclopedia of Environmetrics. John Wiley and Sons, London, UK.

Stewart-Oaten, A., Murdoch, W.W., and Parker, K.R. 1986. Environmental impact assessment: pseudoreplication in time? Ecology 67:929–940.

Underwood, A.J. 1991. Beyond BACI: experimental designs for detecting human environmental impacts on temporal variations in natural populations, Australian Journal of Marine and Freshwater Research 42:569–587.

FIGURE LEGENDS

FIG. 1. Map of the Nysted Offshore Wind Farm study area, showing its position within Denmark (inset). The map shows changes in predicted differences in long-tailed duck numbers across the study area under the spatially-adaptive generalized additive model before and after construction using long-tailed duck abundances adjusted for detectability. Negative differences indicate fewer individuals after construction than before, positive differences indicate more individuals after construction than before. The black '+' and the black open circles represent significant increases or decreases in long-tailed duck numbers under the model. The contour lines represent depth in meters. The position of the wind farm is indicated with a hatched polygon and transect waypoints are indicated with "T".

FIGURE 1

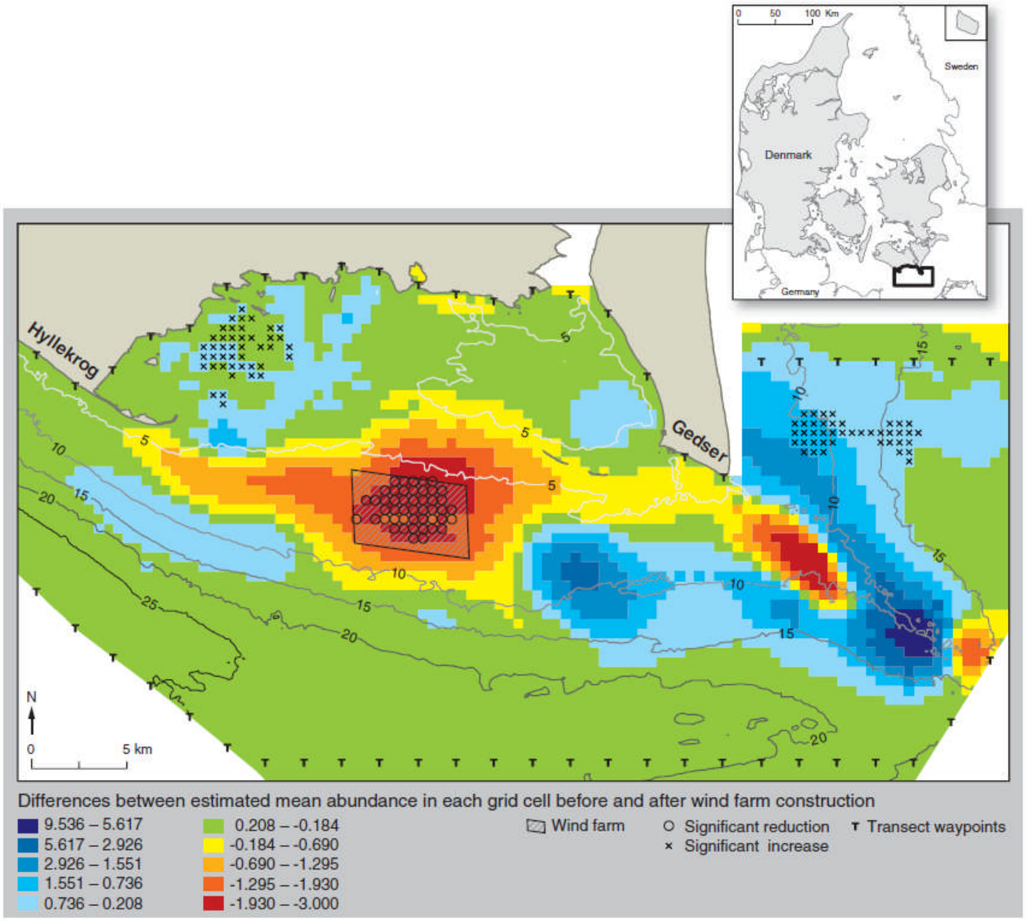

Denmark
Sweden
Germany
0 50 100 Km
Hyllekrog
Gedser
N
0 5 km
Differences between estimated mean abundance in each grid cell before and after wind farm construction
9.536 – 5.617
5.617 – 2.926
2.926 – 1.551
1.551 – 0.736
0.736 – 0.208
0.208 – -0.184
-0.184 – -0.690
-0.690 – -1.295
-1.295 – -1.930
-1.930 – -3.000
Wind farm
Significant reduction
Significant increase
Transect waypoints

APPENDICES

APPENDIX A. Detection function model fitting diagnostics, showing the six detection functions fitted to the original long-tailed duck dataset from Nysted OWF. Perpendicular distance was also included. Survey (index of the 24 surveys conducted during the study), behavior (flocks sitting, swimming, flying, flushing), Beaufort sea state, estimated flock size, observer, and phase of the study were potential covariates in the candidate models. AIC and delta AIC were used as model selection criteria. From the bootstrapping exercise, the proportion of bootstrap replicates in which a given model was selected is also shown.

Key function	Covariates	AIC	ΔAIC	Proportion selected in bootstrap
Hazard rate	Survey, Sea state, Behavior, Group size, Observer	7293.8	0.0	0.56
Half-normal	Survey, Sea state, Behavior, Group size, Observer, Construction	7294.6	0.8	0.37
Half-normal	Survey, Behavior, Group size, Observer	7298.5	4.7	0.07
Hazard rate	Survey, Sea state, Behavior, Observer	7322.4	28.6	0.00
Half-normal	Survey, Sea state, Behavior, Observer, Construction	7324.1	30.3	0.00
Half-normal	Survey, Sea state, Observer, Group size, Construction	7358.5	64.7	0.00

APPENDIX B. Comparisons of pre versus post construction abundance model-based estimates of long-tailed ducks in the Nysted study area, based on observations from aerial surveys. Values show model estimates ± confidence intervals.

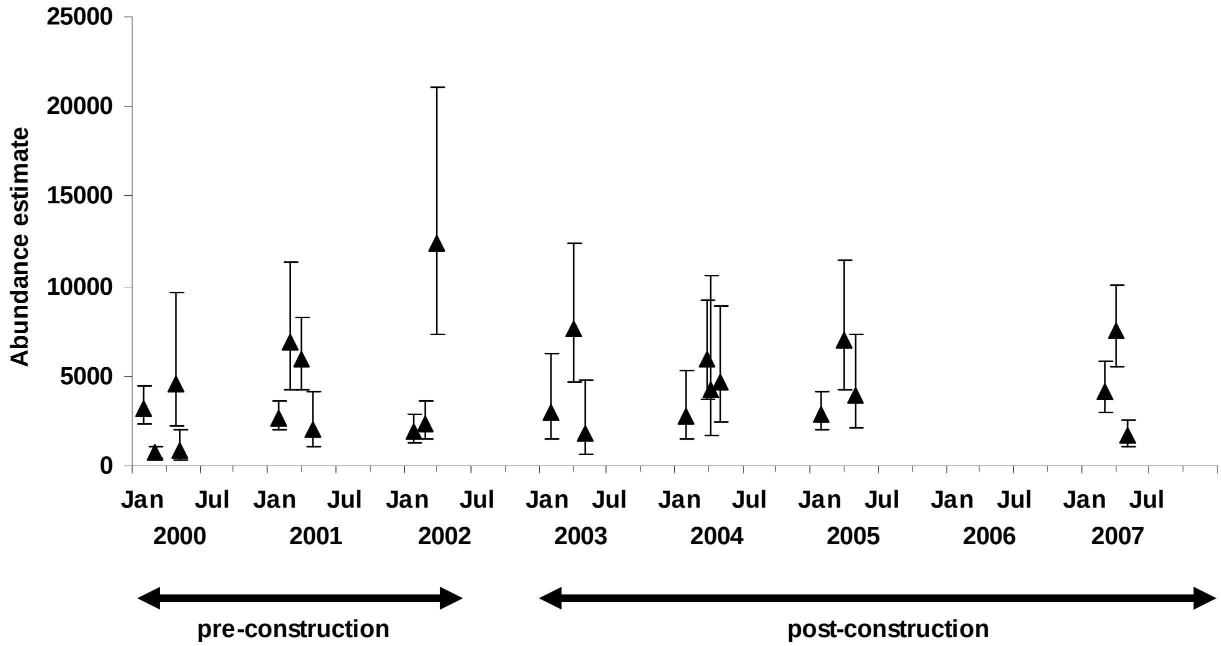

APPENDIX C. The 95% confidence intervals for differences in long-tailed duck numbers across the study area under the spatially-adaptive generalized additive model before and after construction. Two maps showing the lower 95% confidence intervals and the upper 95% confidence intervals respectively for differences in long-tailed duck numbers across the study area under the spatially-adaptive generalized additive model before and after construction using long-tailed duck abundances adjusted for detectability. The black '+' and the black open circles represent significant increases or decreases in long-tailed duck numbers under the model. The contour lines represent depth in meters. The position of the wind farm is indicated with a hatched polygon and transect waypoints are indicated with "T".

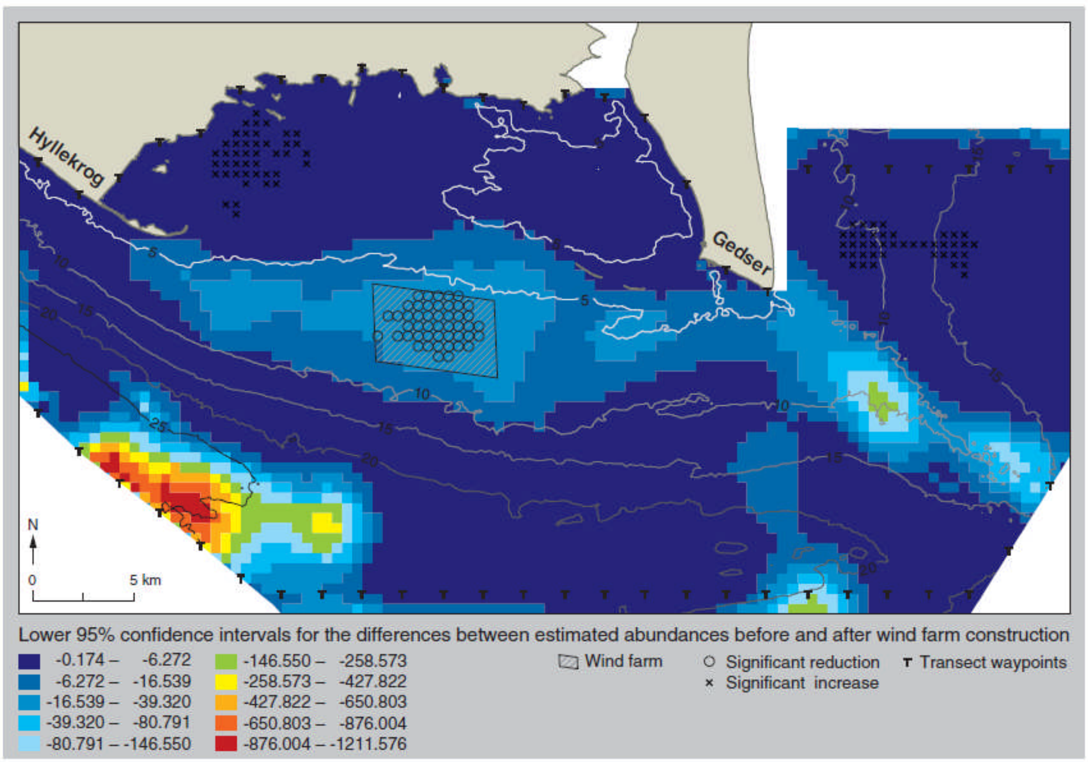

Lower 95% confidence intervals for the differences between estimated abundances before and after wind farm construction

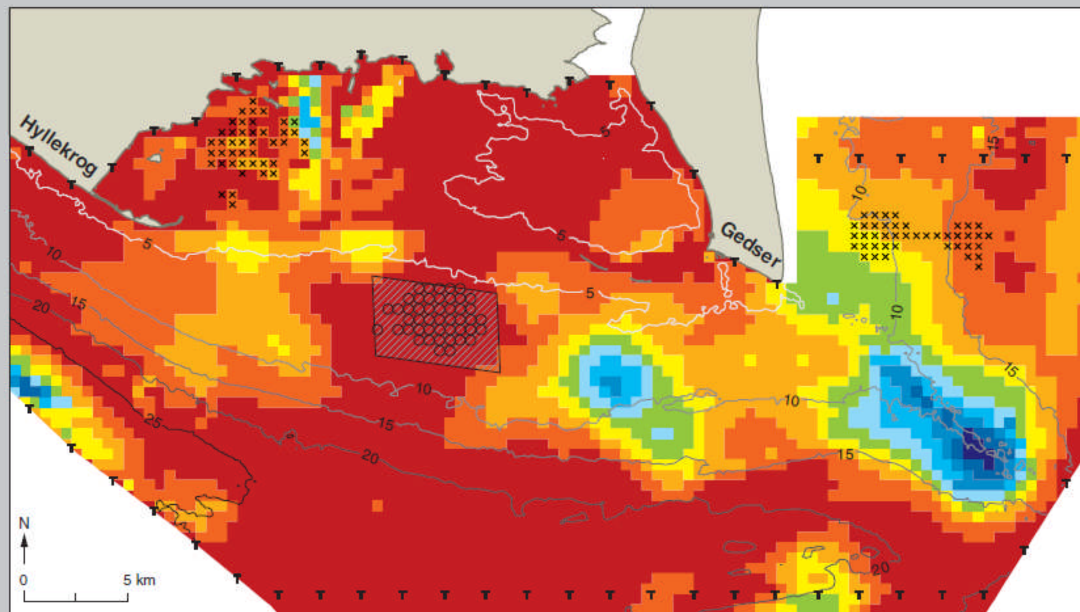

Upper 95% confidence intervals for the differences between estimated abundances before and after wind farm construction

225.288 – 143.080
143.080 – 87.540
87.540 – 53.997
53.997 – 37.109
37.109 – 25.058
25.058 – 16.418
16.418 – 10.248
10.248 – 5.890
5.890 – 2.600
2.600 – -3.322
Wind farm
Significant reduction
Significant increase
Transect waypoints